Pergamon

Tetrahedron: *Asymmetry* 11 (2000) 9–25

TETRAHEDRON:
ASYMMETRY

Enkephalin-based drug design: conformational analysis of O-linked glycopeptides by NMR and molecular modeling

Caroline T. Kriss, Bih-Show Lou, Lajos Z. Szabò, Scott A. Mitchell, Victor J. Hruby and Robin Polt *

Department of Chemistry, The University of Arizona, Tucson, AZ 85721, USA

Received 29 October 1999; accepted 29 November 1999

Abstract

Glycosylation provides an effective means of enhancing penetration of the blood–brain barrier by pharmacologically active peptides. Glycosylated enkephalin analogues demonstrate much greater analgesic effects than their unglycosylated counterparts when administered peripherally. The solution conformations of glycopeptide enkephalin analogues with the sequences H-Tyr-c-[D-Cys-Gly-Phe-D-Cys]-Ser(β-*O*-Glcp)-Gly-NH_2, **2**, and H-Tyr-c-[D-Cys-Gly-Phe-D-Cys]-Ser(α-*O*-Glcp)-Gly-NH_2, **3**, have been determined by NMR and molecular modeling, and were compared to the unglycosylated peptide H-Tyr-c-[D-Cys-Gly-Phe-D-Cys]-Ser-Gly-NH_2, **1**, to determine the impact of glycosylation on peptide conformation. The only observed conformational effects were on the residue of attachment, Ser^6, and on the adjacent Gly^7-amide. This has important implications in peptide-based drug design in that strategically placed glycosylation can improve transport without destruction of the receptor selectivity of a pre-existing non-glycosylated peptide pharmacophore.

1. Introduction

Neuropeptidic drugs hold great promise for the study and control of a wide variety of behavioral disorders thought to be caused by neuropeptide imbalance such as obesity,[1] addiction syndromes,[2] and attention deficit disorders,[3] as well as chronic or neuropathic pain.[4] Synthetic glycopeptides have the potential to replace endogenous neuropeptides.[5] Glycosylation of opioid peptides has proven quite effective as a means to increase serum stability in the bloodstream and penetration of the blood–brain barrier.[5a] Work performed in this laboratory, as well as in two Italian laboratories has shown that glycopeptide-based analgesics can approach, or even surpass, the analgesic effects of morphine.[5a,b,e,g,l,m]

Many naturally occurring proteins are glycosylated, and control of membrane permeability has long been postulated as one of the purposes of protein glycosylation.[6] Explanations of the purpose of the

* Corresponding author. E-mail: polt@u.arizona.edu

0957-4166/00/$ - see front matter
PII: S0957-4166(99)00544-3

carbohydrate include some impact on either the conformation or dynamics of the protein backbone. Shogren, et al.[7a] and Butenhof, et al.[7b] have determined that glycosylation is responsible for the highly extended random coil conformation of mucins. Without the carbohydrate moiety, the protein was much less extended and had a smaller radius of gyration. In determining a more refined picture of the impact of glycosylation, glycopeptides have been studied in hopes that the impact of a carbohydrate on a few residues will be true of much larger molecules. Maeji, et al.,[8] using a tripeptide model of antifreeze glycoprotein, state that the sugar moiety shields the neighboring amino acids from solvent and might hinder the flexibility of the peptide backbone. Fasman, et al.[9] concluded that an *O*-glycosylation stabilizes β-turns in dipeptides. Kahne and Andreotti[10] concluded that *O*-glycosylation dramatically changes the ensemble of conformations of a linear hexapeptide towards a turn structure. The degree of conformational change appears to be tempered by constrained (i.e. cyclic) systems since Kessler, et al.[11] using a cyclic hexapeptide determined that *O*-glycosylation does not affect the conformation of the peptide backbone or side chains.

The synthetic glycopeptide enkephalin analogues **2** and **3** have shown profound and prolonged analgesia when administered peripherally.[5a,f] The unglycosylated peptide **1** showed virtually no activity when administered peripherally. The attachment of a glucose to **1** slightly reduced opiate receptor binding in vitro (radioligand displacement from homogenized rat brain and GPI/MVD assays, Table 1), or when administered by intracerebroventricular injection (i.c.v.) in vivo. However, compared to the unglycosylated compound **1**, the glycopeptides **2** and **3** demonstrated a significant increase in analgesia when administered intraperitoneally (i.p.). Since there was no great difference in serum lifetimes between glycosylated and unglycosylated analogues in this case,[12] the increased analgesia is most likely attributable to greater accessibility to the opiate receptors in the brain. The carbohydrate may provide hydrophilicity, recognition by an active transporter, or possibly induce conformational changes that are key to crossing the blood–brain barrier. While bacterial glycopeptides have been shown to open the blood–brain barrier for the penetration of other drugs, this approach involves inflammation of the endothelial layer and may be considered as somewhat pathogenic.[13]

Table 1
Cyclic glycopeptide analogues

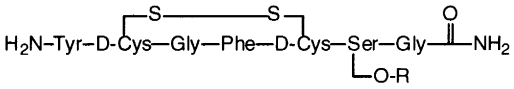

Compound Number	Biological Code	Delta (nM) IC_{50}	Mu (nM) IC_{50}	MVD (nM) IC_{50}	GPI (nM) IC_{50}	R-
1	LSZ-916	6.1	30	5.5	26	H-
2	LSZ-1025	26-45	46-53	13	60	
3	LSZ-52	10	68	34	64	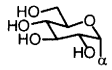

The carbohydrate in this study was attached to a residue pendant to a conformationally restricted (disulfide linkage) turn sequence. Since receptor binding and selectivities were essentially unaffected by

glycosylation, the expectation was that the conformational changes would occur only in the pendant portion (-Ser^6-Gly^7-CONH$_2$) of the molecules. High resolution NMR methods can yield structural information for peptides useful for drug design.[14] Scalar J coupling constants (Karplus relationships) and NOE effects provide the most relevant conformational data for peptides. Unlike larger proteins, smaller peptides in solution are dynamic and undergo conformational change more rapidly than can be observed by NMR, thus these parameters are often time averages of several conformations and great care must be taken in the interpretation of the data.

Molecular modeling was employed to explore the conformational space.[15] Monte Carlo methods were utilized to generate an ensemble of possible low energy conformers for the molecules **1**, **2**, and **3**. Then NMR data was used to refine and/or validate the results.

Since the observed coupling constants could easily have arisen from conformational averaging, only certain NMR data were used to refine the conformational ensembles. For example, coupling constants >9 Hz are maximal for the $^3J_\alpha$H–NH and can only be generated by a dihedral angle near 180°. In this particular case (i.e. coupling constants >9 Hz), the conformational ensemble could potentially be reduced since averaging with conformers of other dihedral angles could only serve to lower the value of the coupling constant. In general, NMR data have been used only to validate the modeling results by looking for agreement between experimental averages and ensemble averages of the J values. In this study, solution conformations of the glycosylated and unglycosylated enkephalin analogues (Table 1) have been studied using NMR and molecular modeling to determine any contributions glycosylation makes to conformation and its consequent increased access to the brain.

1.1. Nuclear magnetic resonance studies

Enkephalin analogues **1**, **2**, and **3** were studied by high resolution (500 MHz) 1D and 2D NMR. Preliminary NMR data were collected on **2** in both water and DMSO-d_6 to compare solvation effects on conformation. Since the NOE pattern was the same for DMSO-d_6 and water, further NMR work was conducted using DMSO-d_6. Because the motional correlation time of the molecule, τ_χ, and the angular Larmor frequency, ω, approached 1, ROESY rather than NOESY experiments were conducted. Complete and unambiguous assignment of all resonances (except for distinction of β from β′ hydrogens) was carried out by the combined analysis of 1D ^{1}H, TOCSY, and ROESY NMR spectra. Chemical shifts varied little from compound to compound. The homonuclear coupling constants were obtained from the highly digitized 1D traces of 2D spectra. The coupling constants (Table 2) yielded no extremes useful for determining conformation.

Initially, ROESY experiments for each compound were conducted with a mixing time of 200 ms. The NOE patterns were virtually identical for both peptide and glycopeptides. No non-trivial NOEs (greater than four residues) were found, which is not unusual for a hexapeptide. Sequential NOEs (αH_i–NH_{i+1}) were examined and were all of approximately equal intensity except for Phe^4, which was much weaker. This absence could denote a greater distance between these two protons, but also might be due to NOEs from two proximal protons having opposite NOE effects. Thus, ROESY experiments were conducted on compound **2** at mixing times of 25, 50, 100, and 300 ms, and the NOE peak buildup rates determined (Table 3). If cancellations were occurring, the peak would be expected to build up and decay quickly. Alternatively, if the protons were distant, buildup should be slow or non-existent. The buildup demonstrated that a sequential NOE for the Phe^4 existed, but built up more slowly than the other NOEs. Since peptides of this size are flexible molecules, it can be safely assumed that they have multiple conformations, and their NOEs as well as coupling constants can be time-weighted averages of these multiple conformations. Assuming that the protons in the cyclic portion of the molecule have similar

Table 2
Vicinal coupling constants for **1**, **2**, and **3**

	$^3J_{NH-\alpha H}$ (Hz)		
	Peptide	**Glycopeptide**	**Glycopeptide**
Residue	**LSZ-916 (1)**	**LSZ-1025 (2)**	**LSZ-52 (3)**
D-cys^2	7.5	7.6	7.8
Gly^3	6.8 5.8	7.4 4.6	6.5 5.6
Phe^4	7.8	7.9	7.9
D-cys^5	7.2	7.4	7.2
Ser^6	7.6	8.0	7.8
Gly^7	6.1 5.8	7.5 5.3	6.1 5.9

relaxation rates, the NOE buildup rates were used to generate average distances between the sequential protons (Table 3) by comparison with the β protons of D-cys^2 which are at a fixed distance of 1.77Å. An NH–NH crosspeak found between Phe^4-D-cys^5 was also observed. The NOE for one of the Gly^3 protons was found to build up and then drop off at a sharp rate and therefore its distance was not calculated.

Table 3
NOE peak buildup and average distances

NOE crosspeak	**NOE Buildup Distance** (Å)	**NOE Calculated Distance** (Å)	**Mol. Mech. Distance** (Å)
Tyr^{1}α-D-cys^{2}NH	1.3	2.0	3.2
D-cys^{2}α-Gly^{3}NH	1.6	1.9	2.2
Gly^{3}α-Phe^{4}NH	1.1	2.0	2.4
Gly^{3}α′-Phe^{4}NH	--[a]	--[a]	3.4
Phe^{4}α-D-cys^{5}NH	0.26	2.6	3.3
D-cys^{5}α-Gly^{7}NH	1.2	2.0	3.1
Ser^{6}α-Gly^{7}NH	--[a]	--[a]	2.6
Phe^{4}NH-D-cys^{5}NH	0.35	2.5	2.3

[a]not obtained due to overlap with diagonal peak.

Two caveats exist for using a ROESY experiment to evaluate NOEs as compared to a NOESY.[16] First, a ROESY employs a spin lock pulse generating an rf field that varies with the offset from the transmitter. As a result the intensity of ROESY peaks can vary based on this offset. Since distances are calculated based on NOE intensity, ignoring this offset might give erroneous estimates of distance. Since

the majority of NOEs evaluated in this experiment are sequential, αH_i to NH_{i+1} and the a protons all have approximately the same transmitter offset which is true of the amide protons as well, any error arising from offset should affect the sequential NOEs equally. Intensity differences between sequential NOEs should then be genuine and could be interpreted as a difference in the average distance between those protons. Care must be taken when interpreting intensity differences for NOEs generated from resonances with different offsets from the transmitter, such as NH–NH or βH–βH resonances.

The second caveat for interpreting ROESY data originates from TOCSY-like (Hartman–Hahn) crosspeaks that arise in J-coupled protons. In a typical ROESY, the diagonal peaks and crosspeaks are opposite in phase. The Hartman–Hahn artifact has the same phase as the diagonal and therefore, when present, leads to a reduction in the intensity of the NOE crosspeak. The danger here is that the NOE crosspeaks occurring between two protons of a known distance used to translate NOE intensity to distance (i.e. nonequivalent geminal protons) are most prone to this effect. With the calibration peak intensity artificially low, calculated NOE distances are likely to be artificially shorter than they would be if the Hartman–Hahn effect was not present. This effect is best minimized by using a relatively small value for rf field strength, i.e. 2 kHz. In the present work, a 3 kHz field strength was used which gave rise to strong NOE crosspeaks, but probably reduced the intensity of the nonequivalent geminal protons used to calculate distances. This will be discussed in the molecular modeling results.

1.2. Monte Carlo simulation

Molecular mechanics techniques were used to seek out the many possible conformations of glycopeptides **2** (β-D-glc) and **3** (α-D-glc), as well as the unglycosylated peptide **1**. The resulting minimized conformational ensembles for each molecule were compared to the NMR data above.

Six Monte Carlo search runs generating 5000 structures each were conducted for each analogue using MacroModel® version 4.5.[17] The AMBER force field[18] and the Generalized Born Solvent Accessible Surface Area (GBSA)[19] solvent model for water were employed. The results of the six runs were then combined, duplicate conformers eliminated, and a 25 kJ/mol energy cutoff employed, yielding a total of 128 unique conformers for **1**, 100 for **2**, and 81 for **3**.

The NMR data were analyzed for possible constraints that could reduce the number of solution conformers representing each analogue. The $^3J\alpha$-H to N–H coupling constants for each amino acid could not be used as constraints since these were all in the average range of 4–9 Hz (Table 2). The pattern of a weak sequential αH_i–NH_{i+1} NOE from Phe[4]-D-cys[5] combined with an NH–NH NOE for these same two residues was in agreement with a β-turn conformation (Fig. 1). The ensembles of conformations for each analogue were screened for the possible β-turn 'types', and type II′ was found to be populated to the extent of 20% for **1**, 27% for **2**, and 44% for **3**.

The average distances for each of the sequential NOEs were generated from the ensemble of conformations and compared to the NOE generated distances for **2** (Table 3); the molecular mechanics results gave larger distances than the distances derived from the NOE averages. The sequential αH_i–NH_{i+1} distances are largely dependent upon ψ for the ith residue since the amide bond is planar. Having measured the sequential proton distance through a 360° rotation of ψ, a distance of 2.0 Å was never obtained. The closest approach of the α proton to the amide proton of the adjacent residue was 2.12 Å when ψ=120°. With four of the six calculated distances shorter than 2.12 Å, it is likely that the β protons of D-cys[2] used to quantify the NOE buildup rates had suffered a Hartman–Hahn effect, which decreased the observed crosspeak intensity and scaled down the distances calculated from this 'known' distance proportionately. What can be interpreted correctly from the NOE data? The trend was that almost all of the sequential NOEs were the same average distance with the exception of Phe[4]. This residue however, displayed an

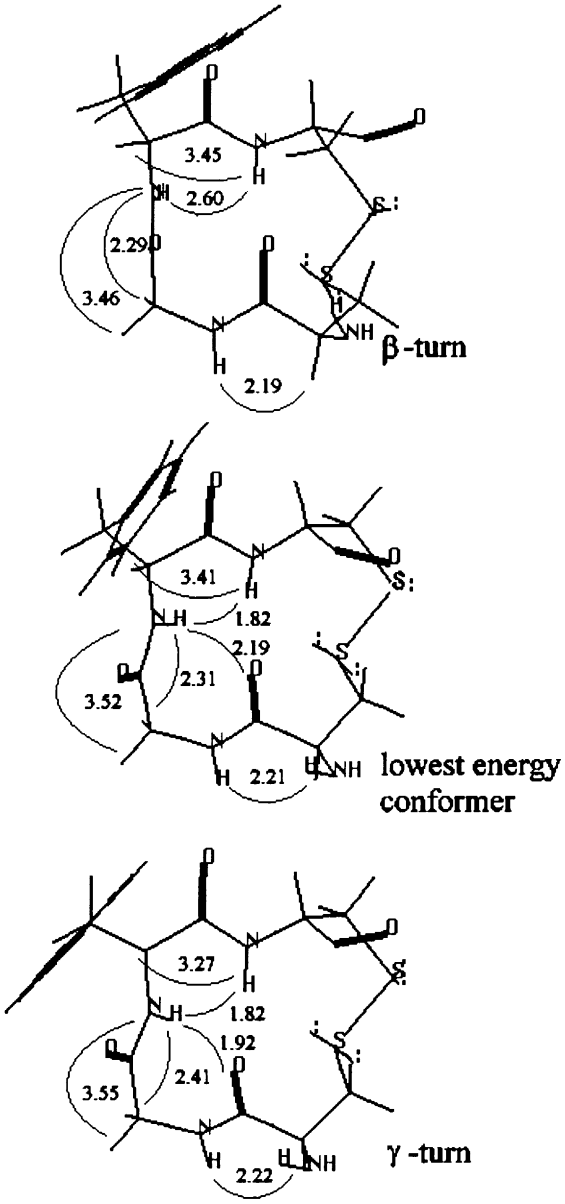

Fig. 1. Representative low energy turns found within the ensembles for **1**, **2** and **3**

NH–NH crosspeak with the adjacent D-cys[5], whose intensity could not accurately be quantified due to offset effects. The Monte Carlo data demonstrated the same trend for the cyclic sequential NOEs, but was somewhat high for the pendant portions of the peptide chain. Also, this method correctly predicted NH–NH proximity for the Phe[4] and D-Cys[5] residues.

Attempts to cluster each of the analogues into families using the XCluster[20] program of MacroModel® were unsuccessful. A variety of criteria were used for overlay, such as all torsion angles, the cyclized backbone torsion angles, all heavy atoms, all backbone heavy atoms, all heavy atoms in the cyclic portion of the backbone, and only the α-carbons; all failed to give good separation into clusters. Since grouping was not possible, another method of summarizing the ensemble of conformers for comparison purposes

was necessary. To evaluate the conformational space sampled by each analogue, Ramachandran-like scatter plots were generated for each residue. Plots for both ϕ vs ψ representing the cyclic backbone (Fig. 2) and pendant backbone (Fig. 3). A plot for χ_1 vs χ_2 and χ_2 vs χ_3 was also generated for Ser^6 to adequately display the effect of α vs β carbohydrate linkage on conformation (Fig. 4). This last plot would be expected to show any *exo*-anomeric effects displayed by the glycoside.

2. Discussion

Before utilizing the molecular mechanics results, some comparison with experimental data were made to ensure their accuracy. Analysis of the ϕ,ψ-plots demonstrated little difference in the torsion angles sampled by the peptide **1**, and glycopeptides **2** and **3**. This was in agreement with the chemical shift data and NOE pattern, which also varied little between peptide and glycopeptides. The NOE buildup results suggested a β-turn conformation, and the existence of about 25% type II′ β-turn conformations in the molecular mechanics results lent further credence to the computational results. The vicinal coupling constants determined by NMR were all averages, also consistent with the molecular mechanics results. As a trend, the molecular mechanics sequential distance averages matched the NOE-derived distances, but were slightly higher than the experimental for the pendant portions. Overall, the ensemble of conformations predicted by molecular mechanics was reasonable; the differences between computational and experimental results can probably be attributed to the inability to accurately determine the amount of time spent in each conformation and therefore weight the ensemble correctly.

All of the analogues gave the identical lowest energy conformation (Fig. 5), which strictly speaking is not a β-turn type II′; it actually resembled a γ-turn. An overlay of the first 40 low energy conformers of **1** (Fig. 6) demonstrated the flexibility in the ring and thus explained its failure to cluster. While the analogues sample a β-turn structure for a significant period of time, exactly how much time is spent in this conformation is not clear.

In the glycopeptide enkephalin analogues studied, the pendant carbohydrate appeared to have virtually no impact on the peptide backbone conformation. In the ϕ,ψ-plots for the conformational space sampled by the peptide backbones in **2** and **3**, only the residue of attachment, Ser^6, and adjacent residue, Gly^7, showed any appreciable variation upon glycosylation. A large difference in the flexibility of Ser^6 and Gly^7 resulted from the β-D-glucoside **2**; and only a slight increase in the space sampled was noted with the α-D-glucoside **3**. This is not surprising considering that residues 2–5 are locked into a cyclic structure by a disulfide bridge; the cyclic portion may be sufficiently constrained that increased steric restrictions introduced by the carbohydrate moiety may have little conformational impact.

The linkage (α vs β) of the carbohydrate seems to limit the influence of the carbohydrate on the peptide backbone conformation. The α-anomer, **3**, has much less influence than the β-anomer, **2**. This may be because the flexibility of the carbohydrate is limited due to the anomer. In examining the χ_2 vs χ_3 scatter plots for Ser^6, the α connection can only achieve a gauche plus conformer for χ_3 (the serine oxygen to anomeric carbon torsion angle), while the β connection achieves both gauche plus and minus conformers about this bond. This also has some important implications to the understanding the core regions of naturally occurring O-linked glycoproteins, the great majority of which contain an α-linked GalNAc residue attached to serine or threonine.[21]

If the cyclic portion of **2** is positioned and labeled as in a β-turn, with the D-cys^2 as position i and the D-cys^5 as position i+3, and the molecule is turned so that position i shields position i+3 from sight (and i+1 shields i+2), then a right (obverse) and left (reverse) face can be defined (Fig. 7). In looking at the general shape of the molecule, it was noted that the exocyclic backbone segments with respect to the

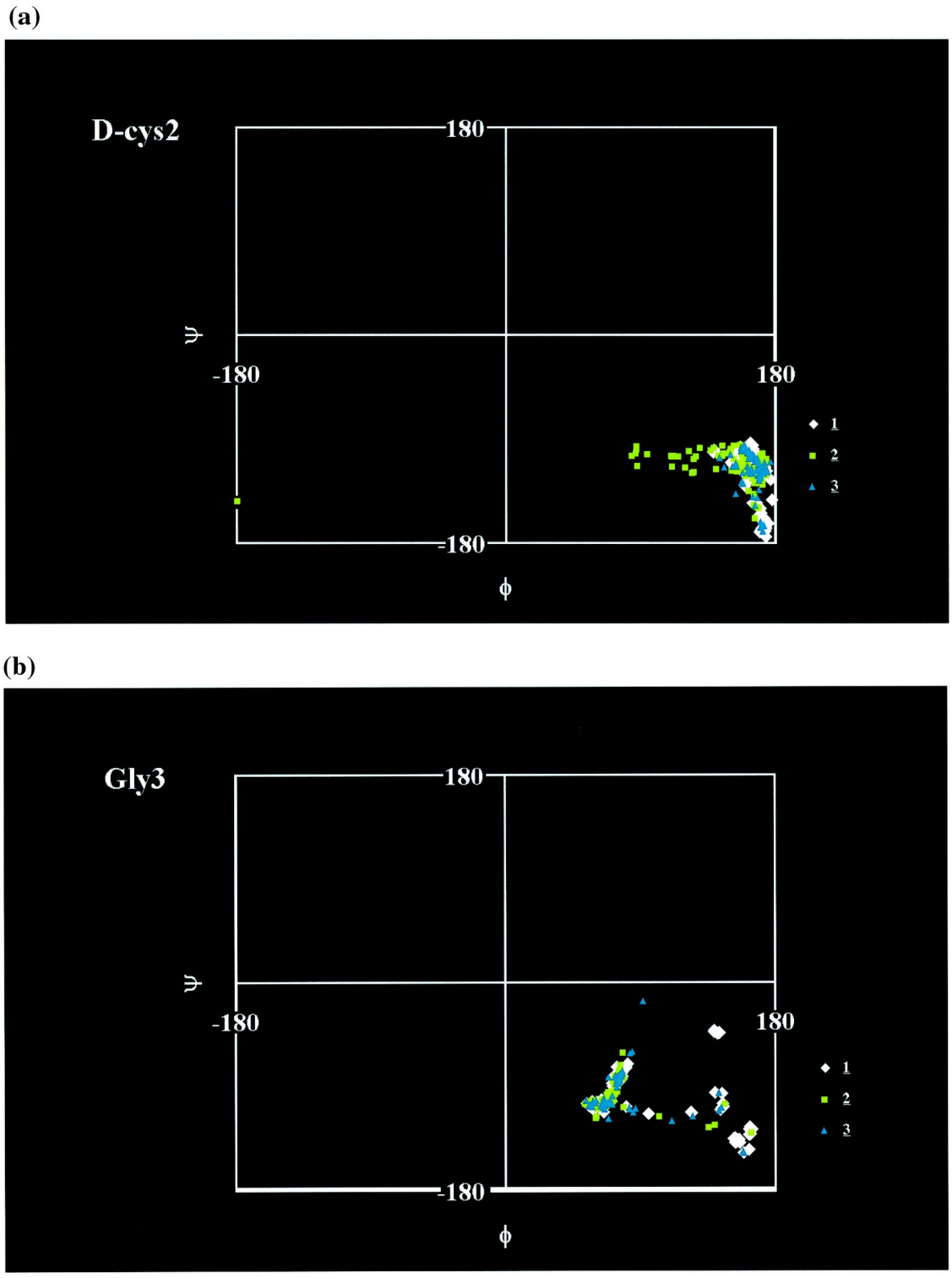

Fig. 2 Scatter plots of the ϕ vs ψ angles for the ensemble of conformers for each residue in the cyclic portion of **1**, **2**, and **3**: (a) D-cys[2], (b) Gly[3], (c) Phe[4], (d) D-cys[5]

(c)

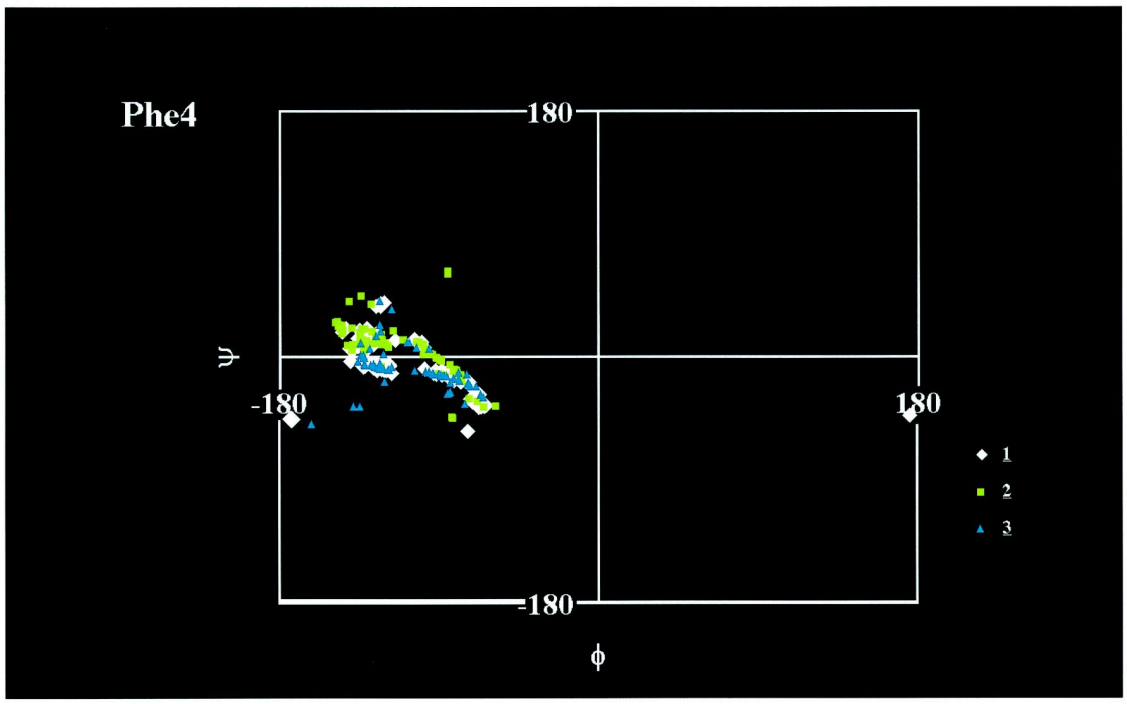

(d)

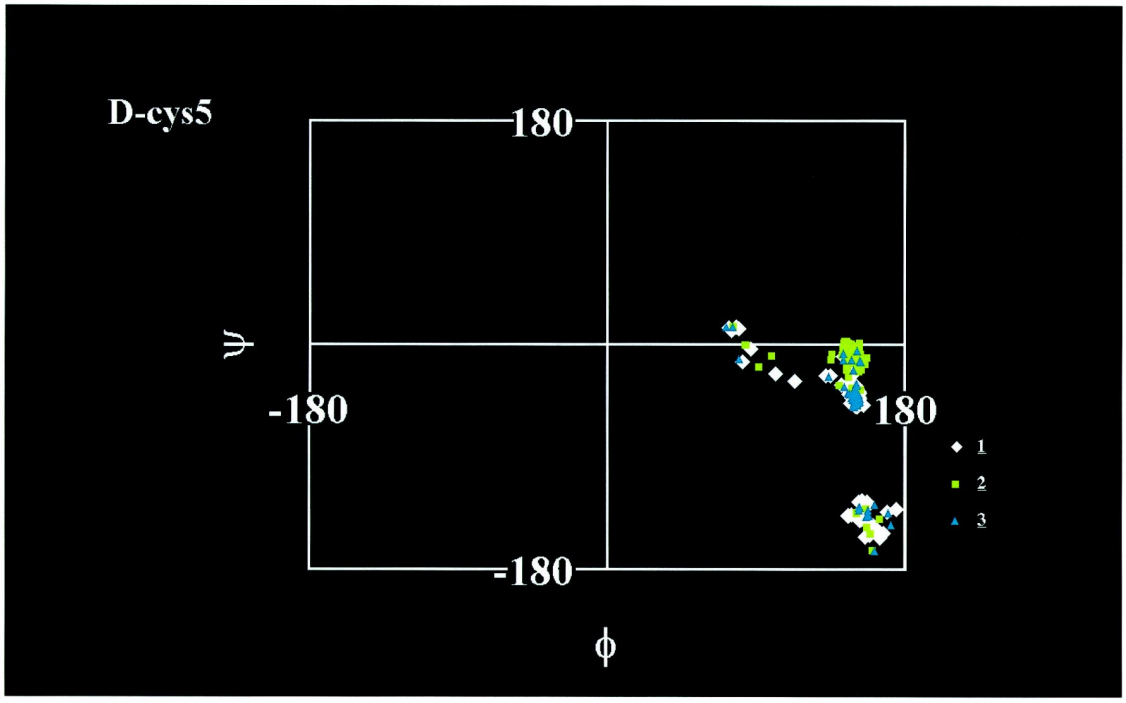

Fig. 2 (continued)

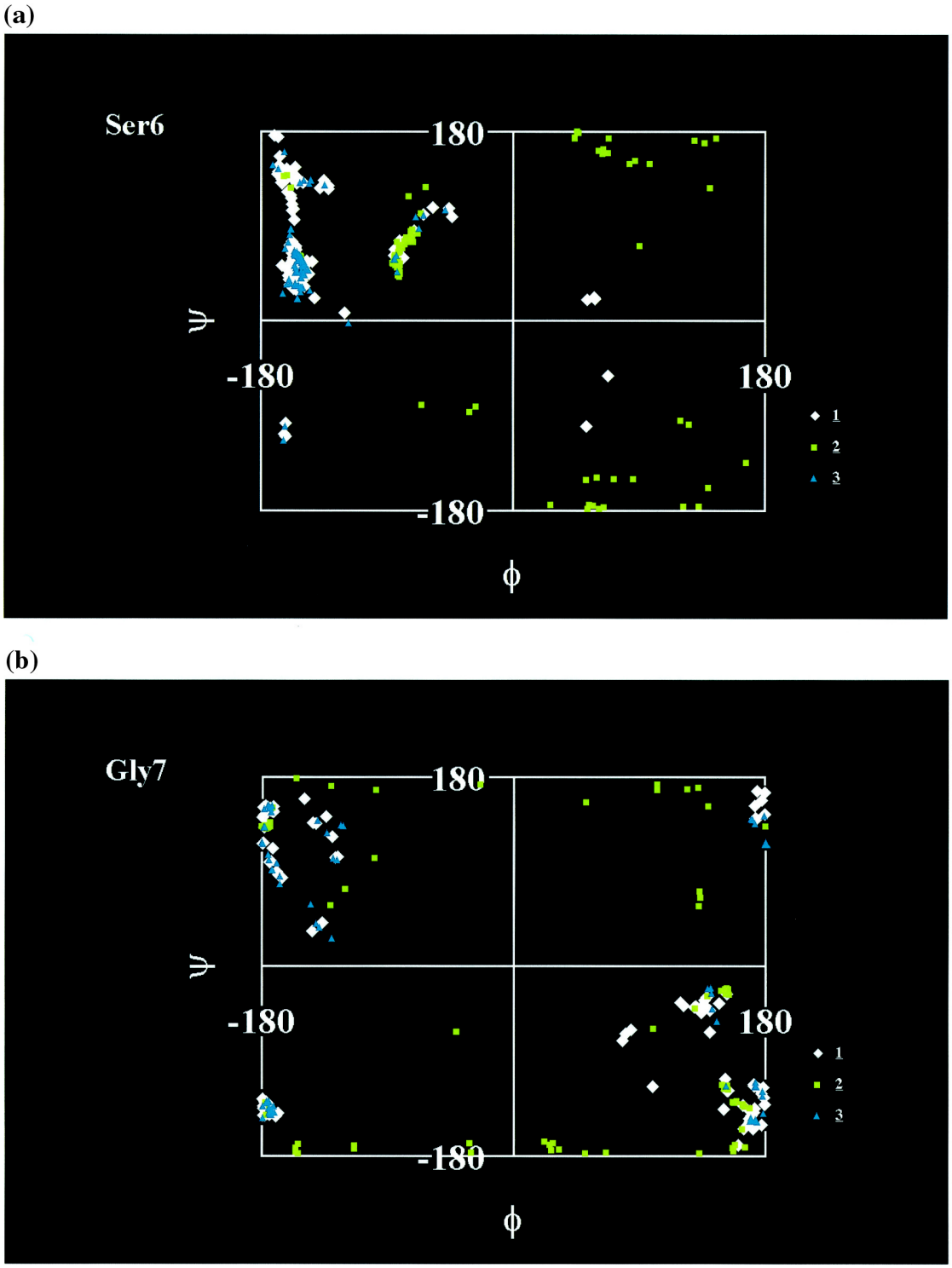

Fig. 3. Scatter plots of ϕ vs ψ angles for the ensemble of conformers for each residue in the pendant portion of **1**, **2**, and **3**: (a) Ser^{6}, (b) Gly^{7}

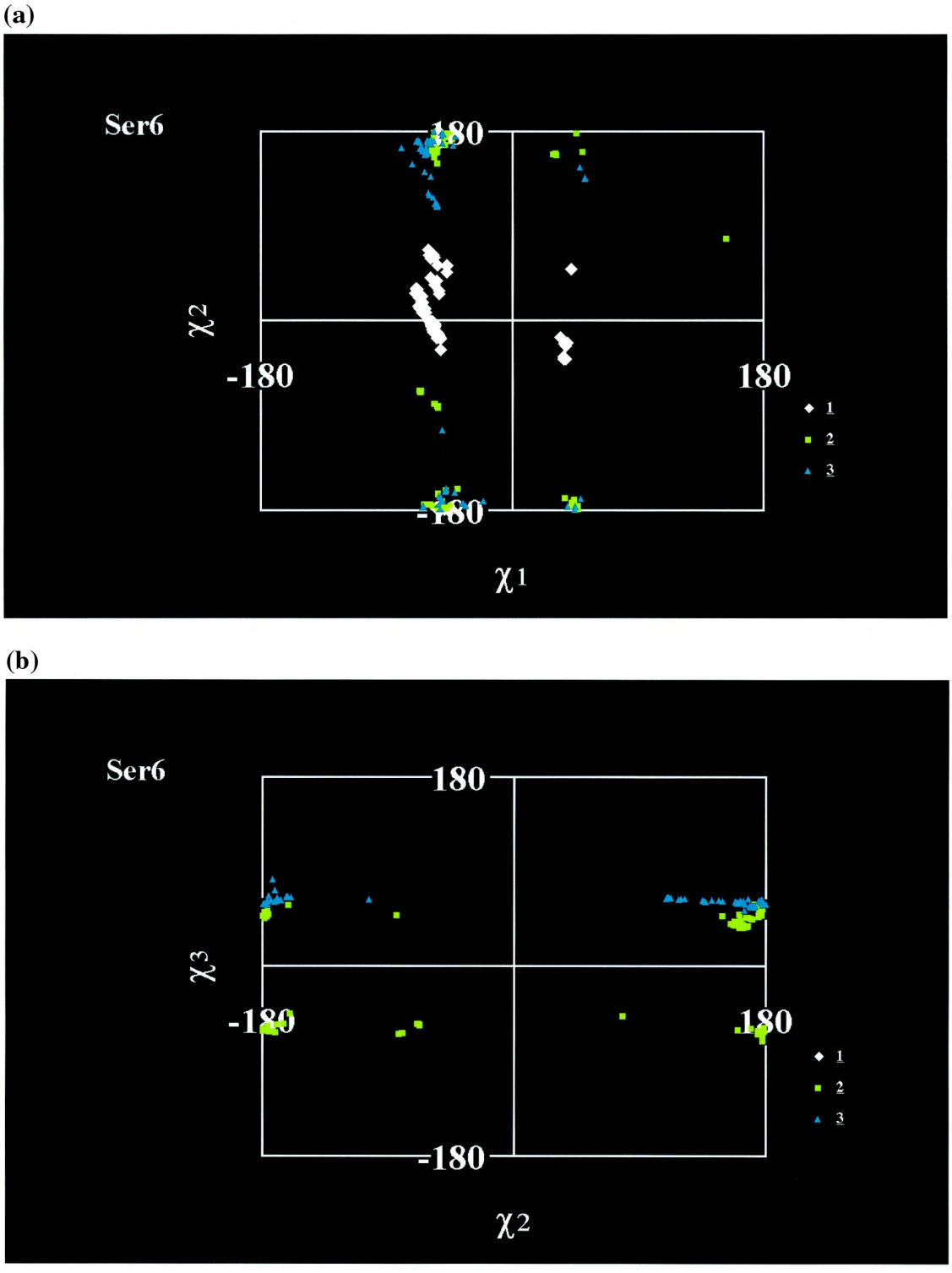

Fig. 4. Scatter plots of the Ser[6] χ_1 vs χ_2 (unglycosylated **1**, β-glycoside, **2**, and α-glycoside, **3**) and χ_2 vs χ_3 (**2** and **3** only)

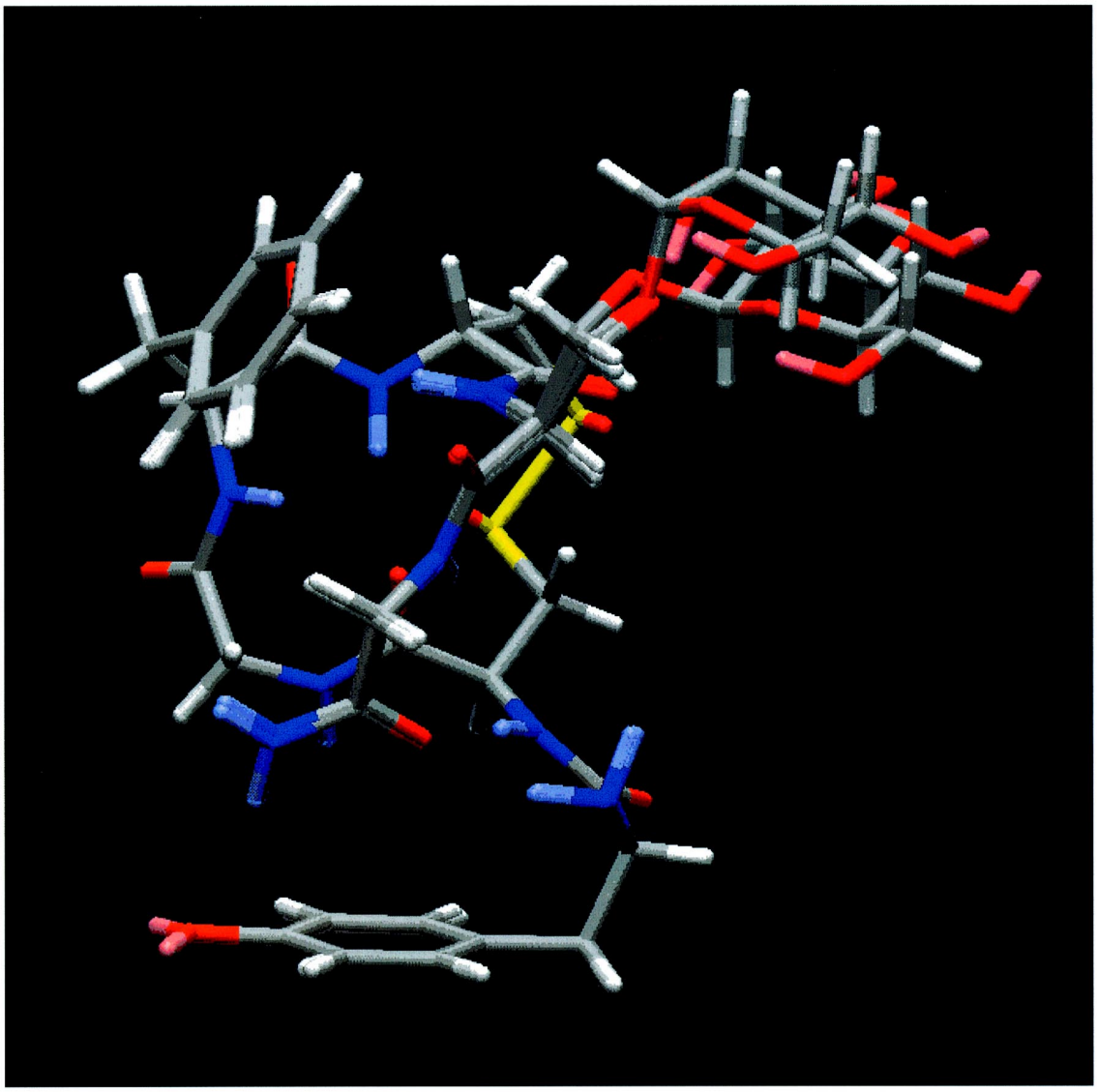

Fig. 5. Overlay of the minimum energy conformations of **1**, **2**, and **3**

cyclic portion all fall to the obverse face of the turn region (lavender surface). This is in partial agreement with the conformation of [Leu]^5-enkephalin (H-Tyr-Gly-Gly-Phe-Leu-OH).[22] As determined by X-ray diffraction, the backbone of [Leu]^5-enkephalin was shown to form a 'β-bend' approximating a plane with the Tyr^1 and Phe^4 side chains on one face of the plane, and the Leu^5 side chain on the opposite face. While the Tyr^1 is on the obverse face in **1**, **2**, and **3**, as well as [Leu]^5-enkephalin, it is difficult to make a direct comparison between the pendant dipeptide group in the peptides **1**, **2**, and **3**, and the side chain of Leu^5. To correspond directly to the [Leu]^5-enkephalin conformation, the D-cys^5 side chain should be on the reverse face, but the substitution of a D-amino acid for Leu^5 reverses this orientation.

Of particular interest is the presence of the C-terminal pendant dipeptide on the obverse face, which could potentially produce undesirable interactions with the pharmacophore (Tyr^1-Phe^4). Alternatively, this group can mask the polar backbone carbonyls by intramolecular H-bonding to render the cyclic

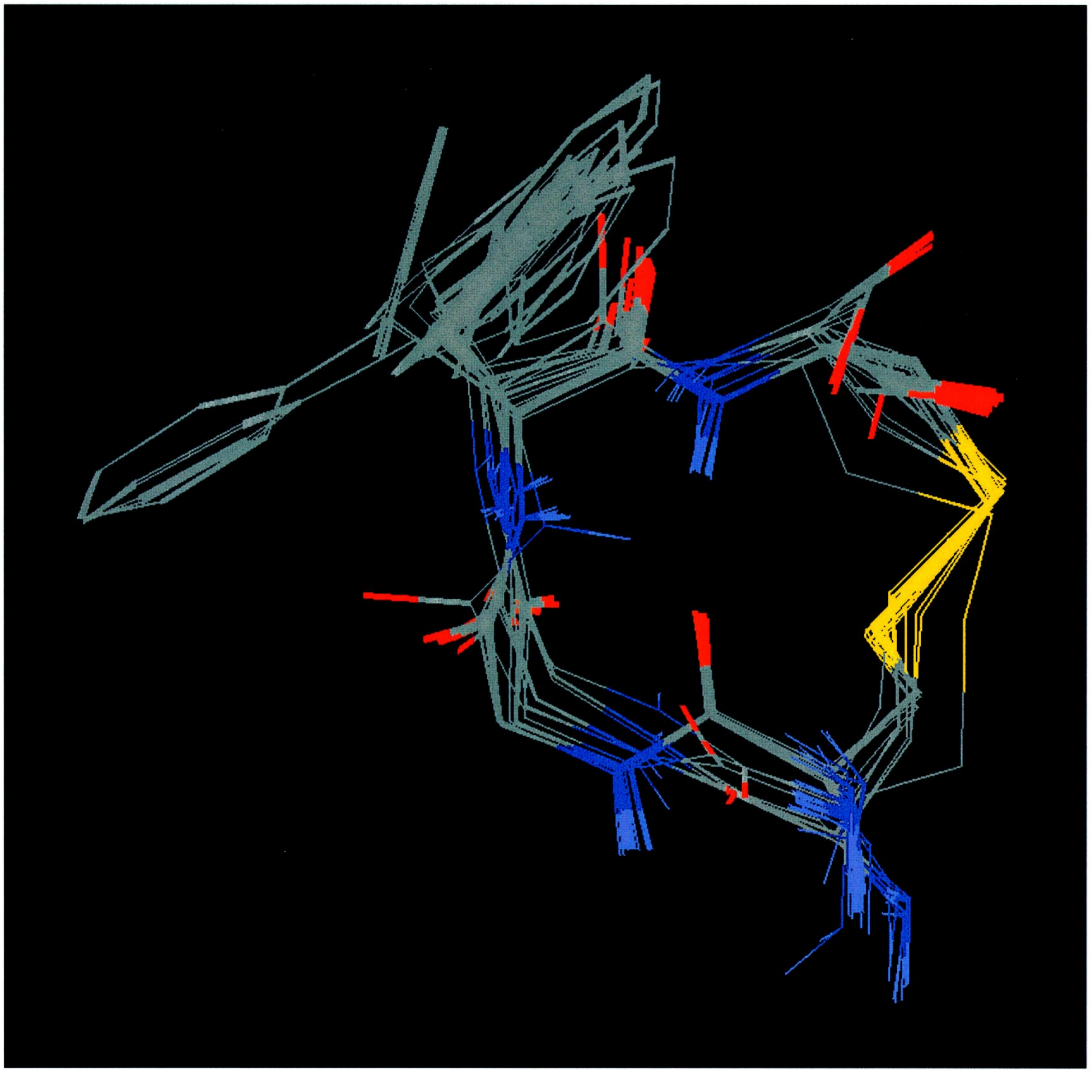

Fig. 6. Overlay of the 40 lowest energy ring conformers of **1**

peptide more lipophilic. Since these glycopeptides have been shown to penetrate the blood–brain barrier, the folding of glycopeptides **2** and **3** into amphipathic structures facilitates transport of these drugs across biological membranes, e.g. by absorptive endocytosis[23] (Fig. 8).

3. Conclusions

The peptide and glycopeptide enkephalin analogues sample the same conformational space. The carbohydrate has virtually no impact on the cyclic portion of the peptide backbone, but does influence the exocylic portion — its residue of attachment, Ser^6, and the Gly^7 adjacent to it. Given a non-cyclic peptide backbone, it may demonstrate more influence, particularly turn induction and stabilization as found by Kahne[11] and by Fasman[10]. The carbohydrate only influences the exocyclic portion of the

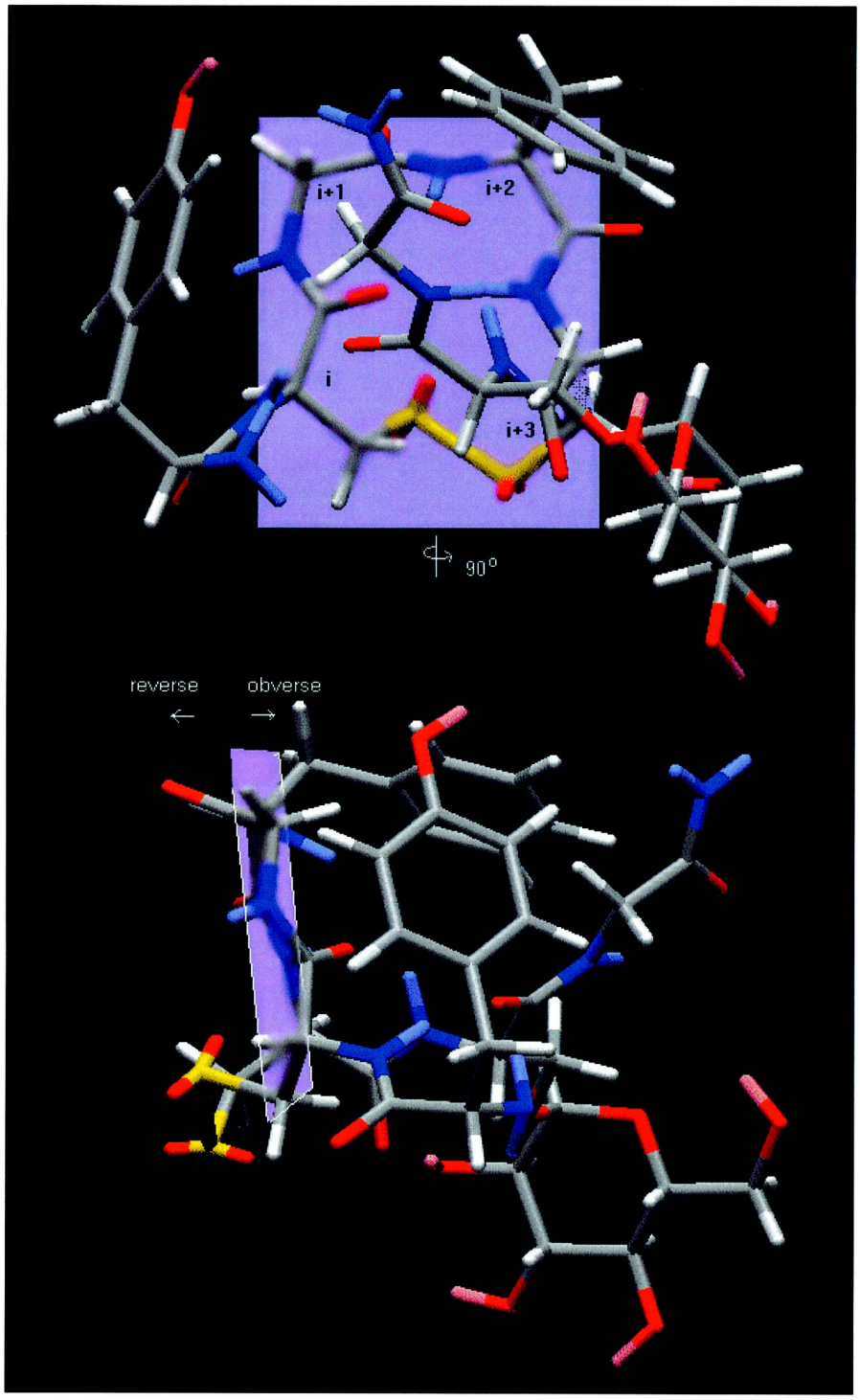

Fig. 7. Pendant portions vs cyclic portions of **2**: obverse vs reverse faces of the turn

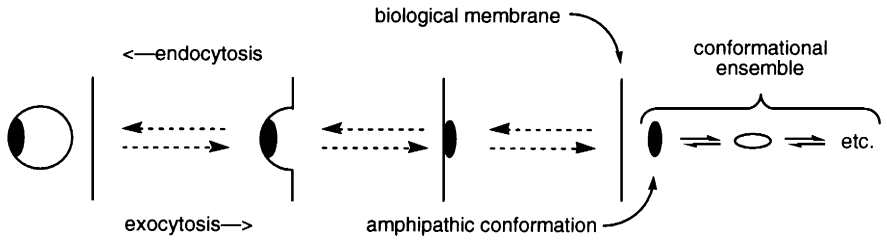

Fig. 8. Absorptive endocytosis is enhanced by amphipathic conformations of glycopeptides

backbone when it has the flexibility of a β-linkage; an α-linkage is much more constrained and distorts the exocyclic backbone less. The C-terminal exocyclic portions of the molecule including the sugar moiety are displayed on the obverse face of the cyclic portion (Fig. 7). This fact may be useful if one considers the backbone ring as a scaffold for the attachment of pharmacophoric side chains. The possibility of directing portions of a peptide to one face of a flexible ring using D vs L amino acids can be of great value in designing the shape of glycopeptide drugs. Presently, glycosylation may be used to improve molecular properties important to drug delivery without impacting carefully designed peptide pharmacophores through the judicious use of amino acid substitution, cyclization, and/or α-linkage. With further exploration, the effect of glycosylation on transport properties may be determined, and conformation-inducing properties may be simultaneously exploited to shape glycopeptides to target particular peptide receptors and increase bioavailability simultaneously.

4. Experimental

4.1. General methods

Peptide resins and FMOC-amino acids were purchased from Bachem (Torrence, CA). All air- and moisture-sensitive reactions were performed under an argon atmosphere in flame-dried flasks. THF was dried and deoxygenated over benzophenone/Na(0)–K(0), CH_2Cl_2 dried over P_2O_5, CH_3CN dried over CaH_2, and all solvents were freshly distilled under an argon atmosphere prior to use. Glycopeptide assembly via FMOC chemistry was performed manually using a sintered-glass fritted vessel with argon as an agitant, or in a fritted vessel with argon agitant and mechanical shaking in a Protein Technologies Sonata using automation. Flash chromatography was performed on 400–230 mesh silica gel 60 (E. Merck No. 9385). All compounds described were at least 95% pure based on ^1H and ^{13}C NMR and confirmed by elemental analyses in certain cases.

4.2. Synthesis and isolation of glycopeptides

The FMOC-amino acid glycosides[24] were synthesized from their corresponding L-serine Schiff bases and the appropriate bromo-sugar (either peracetates or perbenzoates). Glycosylations were performed under Koenigs–Knorr conditions with AgOTfl as a catalyst for β-glycosides and $AgClO_4$ for α-glycosides. Standard deprotection and reprotection afforded the FMOC-amino acid glycosides ready for glycopeptide synthesis in excellent yields. Peptide synthesis utilized deprotections with 25% piperidine in DMF and residue couplings with BOP/HOBt in NMP.[25] The carbohydrate ester protection was removed while on the resin via treatment with $H_2N–NH_2 \cdot H_2O$ in MeOH. Cleavage was accomplished with TFA and appropriate scavengers over 2 h. Ether precipitation followed by purification on a Vydek preparative C_{18} reversed-phase column (Separations Group, Hesperia, CA) gave either the pure reduced forms,

or pure *S*-protected forms. The acetamidomethyl group was removed with $Hg(OAc)_2$ and H_2S, and cyclization was promoted with $K_3Fe(CN)_6$ at a pH of 8.5 under diluting conditions. The crude cyclic samples were re-purified as before. A detailed presentation of both glycoside and glycopeptide synthesis will be published separately.

4.3. NMR measurements

All experiments were carried out at 298 K with a Bruker AM 500 spectrometer equipped with an Aspect 3000 computer and a 5 mm inverse detection probe. Sample concentrations were ~5 mg/0.4 ml analogues in DMSO-d_6. The z-filtered ^{1}H TOCSY[26] spectra were recorded using a relaxation delay of 1 s between the subsequent transients, and the isotropic mixing period (MLEV-17) was set to 60 ms. Thirty-two scans were acquired for each of 512 experiments, and 4096 points were recorded in the acquisition dimension (F2). The z-filtered delay, $T_{z,}$ of 15 ms was randomly varied to obtain pure absorption phase data. Quadrature detection in the F1 dimension was achieved by time-proportional phase incrementation (TPPI). The spectral width was 5435 Hz, resulting in initial digital resolution of 2.6 Hz per point in F2. Zero-filling in both F1 and F2 and multiplication with a square cosine function was performed prior to 2D Fourier transformation.

To improve the definition of the absorption spectrum, a final digital resolution of 0.3 Hz per point was achieved by inverse Fourier transformation, zero-filling, and back transformation of selected traces. The conformationally important homonuclear vicinal coupling constants were determined by the highly digitized (32 K) 1D traces of z-filtered TOCSY spectra and 1D ^{1}H spectra.

ROESY experiments[27] were carried out in reverse configuration using the decoupler for ^{1}H pulsing. Decoupler power was attenuated to give a 90° pulse of 75 μs (spin-lock field strengths of 3333 Hz). The duration of CW spin-lock pulse was 200 ms. Five hundred twelve experiments with 64 transients were carried out. Zero-filling in both F1 and F2 and multiplication with squared cosine function were performed prior to 2D Fourier transformation.

The buildup ROESY experiments were conducted in the same configuration and at the same decoupler power, with mixing times of 25, 50, 100, and 300 ms. 750 experiments with 16 transients were carried out. Zero-filling and a sinebell function were applied in both dimensions prior to Fourier transformation.

Six Monte Carlo search runs generating 5000 structures each were conducted for each analogue using MacroModel® version 4.5.[15] The AMBER force field[16] and GBSA[17] solvent model for water were employed. During each run, a crude conjugate gradient minimization of 500 iterations was performed and structures whose energy was within 50 kJ/mol of the lowest one found were saved. The resulting conformers were then extensively minimized for 10 000 iterations, and again structures within 50 kJ/mol of the lowest saved. The results of the six runs were then combined, duplicate conformers eliminated, and a 25 kJ/mol energy cutoff employed.

Acknowledgements

We would like to thank the U.S. Public Health Service National Institute for Drug Abuse (grant DA06284) and the National Science Foundation (grant CHE-9526909) for their support. We would also like to thank Protein Technologies of Tucson, AZ, for the loan of a prototype automated solid-phase peptide synthesizer.

References

1. Stallone, D. D.; Stunkard, A. J. *Obesity. Biological Bases of Brain Function and Disease*; Frazer, A.; Molinoff, P.; Winokur, A., Eds.; Raven Press: New York, 1994; pp. 386–403.
2. Zlokovic, B. V.; McComb, J. G.; Perlmutter, L.; Weiss, M. H.; Davson, H. Neuroactive Peptides and Amino Acids at the Blood–Brain Barrier: Possible Implications for Drug Abuse. In *Bioavailability of Drugs to the Brain and the Blood–Brain Barrier*; Frankenheim, J.; Brown, R. M., Eds.; U. S. Dept. of Health and Human Services: Rockville, MD, 1992; pp. 26–42.
3. De Wied, D. *Ann. NY Acad. Sci*. **1977**, *297*, 263–274.
4. Hughes, J.; Smith, T. W.; Kosterlitz, H. W.; Fothergill, L. A.; Morgan, B. A.; Morris, H. R. *Nature* **1975**, *258*, 577–579.
5. (a) Polt, R.; Porreca, F.; Szabo, L.; Bilsky, E.; Davis, P.; Abbruscato, T.; Davis, T.; Horvath, R.; Yamamura, H.; Hruby, V. *Proc. Natl. Acad. Sci. USA* **1994**, *91*, 7114–7118. (b) Tomatis, R.; Marastoni, M.; Balboni, G.; Guerrini, R.; Capasso, A.; Sorrentino, L.; Santagada, V.; Caliendo, G.; Lazarus, L.; Salvadori, S. *J. Med. Chem.* **1997**, *40*, 2948–2952. (c) Kihlberg, J. Ahman, J.; Walse, B.; Drakenberg, T.; Nilsson, A.; Soderberg-Ahlm, C.; Bengtsson, B.; Olsson, H. *J. Med. Chem.* **1995**, *38*, 161–169. (d) Fisher, J. F.; Harrsion, A. W.; Bundy, G. L.; Wilkinson, K. F.; Rush, B. D.; Ruwart, M. J. *J. Med. Chem.* **1991**, *34*, 3140–3143. (e) Rodriguez, R. E.; Rodriguez, F. D.; Sacristan, M. P.; Torres, J. L.; Valencia, G.; Garcia, A. *Neuroscience Lett.* **1989**, *101*, 89–94. (f) Polt, R. L.; Porecca, F.; Szabo, L.; Hrubv, V. J. *Glycoconj. J.* **1993**, *10*, 261. (g) Bardaji, E.; Torres, J. L.; Clapes, P.; Albericio, F.; Barany, G.; Rodriguez, R. E.; Sacristan, M. P.; Valencia, G. *J. Chem. Soc., Perkin Trans. 1* **1991**, 1755–1759. (h)Varga-Degterdarovic, L.; Horvat, S.; Chung, N. N.; Schiller, P. W. *Int. J. Pept. Protein Res.* **1992**, *39*, 12–17. (i) Lavielle, S.; Ling, N.; Brazeau, P.; Benoit, R.; Wasada, T.; Harris, D.; Unger, R.; Guillmen, R. *Biochem. Biophys. Res. Commun.* **1979**, *91*, 614–622. (j) Geiger, R.; Koning, W.; Sandow, J. *Peptides: Chemistry, Biology, Interactions with Proteins*; Penke, B.; Torok, A., Eds.; Proceedings of the 50th Anniversary Symposium of the Nobel Prize of Albert Szent-Gyorgi; Walter de Gruyter & Co.: Berlin, 1988; pp. 385–392. (k) Gobbo, M.; Biondi, L.; Filira, F.; Scolaro, B.; Rocchi, R.; Piek, T. *Int. J. Pept. Protein Res.* **1992**, *40*, 54–61. (l) Negri, L.; Lattanzi, R.; Tabacco, F.; Scolaro, B.; Rocchi, R. *Brit. J. Pharm.* **1998**, *124*, 1516–1522. (m) Negri, L.; Lattanzi, R.; Tabacca, F.; Orrù, L.; Severini, C.; Scolaro, B.; Rocchi, R. *J. Med. Chem.* **1999**, 42, 400–404.
6. Montreuil, J. *Adv. Carbohydr. Chem. Biochem.* **1980**, *37*, 157–223.
7. (a) Shogren, R.; Gerken, T. A.; Jentoft, N. *Biochemistry* **1989**, *28*, 5525–5536. (b) Butenhof, K. J.; Gerken T. A. *Biochemistry* **1993**, *32*, 2650–2663.
8. Maeji, N. J.; Inoue, Y.; Chujo, R. *Biopolymers* **1987**, *26*, 1753–1767.
9. Hollosi, M.; Perczel, A.; Fasman, G. D. *Biopolymers*, **1990**, *29*, 1549–1564.
10. Andreotti, A. H.; Kahne, D. *J. Am. Chem. Soc*. **1993**, *115*, 3352–3353.
11. Kessler, H.; Matter, H.; Gemmecker, G.; Kottenhahn, M.; Bats, J. W. *J. Am. Chem. Soc*. **1992**, *114*, 4805–4818.
12. Williams, S. A.; Abbruscato, T. J.; Szabo, L.; Polt, R.; Hruby, V.; Davis, T. P. *Biology and Physiology of the Blood–Brain Barrier*; Couraud & Scherman, Eds.; Plenum Press: New York, 1996; pp. 69–77.
13. Spellerberg, B.; Prasad, S.; Cabellos, C.; Burroughs, M.; Cahill, Pl.; Toumanen, E. *J. Exp. Med.* **1995**, *182*, 1037–1044.
14. (a) Gunther, H. *NMR Spectroscopy*; John Wiley & Sons: New York, 1995. (b) Cavanagh, J.; Fairbrother, W. J.; Palmer III, A. G.; Skelton, N. J. *Protein NMR Spectroscopy Principles and Practice*; Academic Press: San Diego, 1996. (c) Wuthrich, K. *NMR of Proteins and Nucleic Acids*; John Wiley & Sons: New York, 1986.
15. Duben, A. J.; Bush, C. A. *Arch. Biochem. Biophys.* **1983**, *225*, 1–15.
16. Bax, A.; Davis, D. G. *J. Magn. Reson*. **1985**, *63*, 207–231.
17. Mohamadi, F.; Richards, N. G.; Guida, W. C.; Liskamp, R.; Lipton, M.; Canfield, C.; Chang, G.; Hendrickson, T.; Still, W. C. *J. Comp. Chem.* **1990**, *11*, 440–467.
18. Glennon, T. M.; Zheng, Y. J.; LeGrand, S. M.; Shutzberg, B. A.; Merz Jr., K. M. *J. Comp. Chem.* **1994**, *15*, 1019–1040.
19. Still, W. C.; Tempczyk, A.; Hawley, R. C.; Hendrickson, T. *J. Am. Chem. Soc.* **1990**, *112*, 6127–6129.
20. Shenkin, P. S.; McDonald, D. Q. *J. Comp. Chem*. **1994**, *15*, 899–916.
21. (a) Hounsell, E. F.; Davies, M. J.; Renouf, D. V. *Glycoconjugate J*. **1996**, *13*, 19–26. (b) Montreuil, J. *Adv. Carb. Chem. Biochem.*, **1980**, *37*, 157–223.
22. Smith, G. D.; Griffin, J. F. *Science* **1978**, *199*, 1214–1216.
23. Egleton, R. D.; Mitchell, S. A.; Polt, R.; Hruby, V. J.; Davis, T. P. *Brain Res.*, submitted for publication.
24. Szabo, L.; Ramza, J.; Langdon, C.; Polt, R. *Carbohydr. Res*. **1995**, *274*, 11–28.
25. Polt, R.; Szabo, L.; Treiberg, J.; Li, Y.; Hruby, V. *J. Am. Chem. Soc*. **1992**, *114*, 10249–10258.
26. (a) Bax, A.; Davis, D. G. *J. Magn. Reson*. **1985**, *65*, 355–360. (b) Braunschweiler, L.; Ernst, R. R. *J. Magn. Reson*. **1983**, *53*, 521–528.
27. Kessler, H.; Griesinger, C.; Wagner, K. *J. Am. Chem. Soc*. **1987**, *109*, 6927–2933. (c) Kover, K. E.; Prakash, O.; Hruby, V. J. *J. Magn. Reson. Chem.* **1993**, *31*, 231–237.